J. Phys. B: At. Mol. Opt. Phys. 24 (1991) 3479–3490. Printed in the UK

Differential cross sections for electronic excitation of molecular hydrogen using the R-matrix method

Susan E Branchett†, Jonathan Tennyson† and Lesley A Morgan‡

† Department of Physics and Astronomy, University College London, London WC1E 6BT, UK

‡ Computer Centre, Royal Holloway and Bedford New College, Egham, Surrey TW20 0EX, UK

Received 12 February 1991

Abstract. Differential cross sections are calculated for electron–H_2 collisions for scattering energies up to 20 eV. Elastic scattering and excitation from the ground, $X\,^1\Sigma_g^+$, to the lowest six excited electronic states, $b\,^3\Sigma_u^+$, $a\,^3\Sigma_g^+$, $c\,^3\Pi_u$, $B\,^1\Sigma_u^+$, $E,F\,^1\Sigma_g^+$ and $C\,^1\Pi_u$, is explicitly considered for all total symmetries up to and including $^2\Phi_g$ for a single fixed H_2 geometry. The target states are represented using a full configuration interaction treatment within a basis of Slater-type orbitals optimized to give accurate vertical excitation energies. Results are presented for both resonant and non-resonant differential cross sections. Comparison is made with the available experimental and theoretical data. Excellent agreement is obtained for elastic differential cross sections; agreement for the inelastic differential cross sections is only moderate. Possible improvements to these calculations are discussed.

1. Introduction

The study of differential cross sections for electronic excitation processes is an important test of theoretical models because the available non-resonant experimental data for differential cross sections are far more accurate than for integrated cross sections. This is due to the need to extrapolate differential cross section data to 0° and 180° prior to integration. It is only by studying the differential cross sections in the resonant energy region that the observed angular distributions of the resonance series can be understood.

Experimental work on integrated and differential cross sections, for various excitation processes, has been reviewed recently by Tawara *et al* (1990) for non-resonant measurements.

There have also been studies on resonant electron–H_2 collisions. Early work on this problem was reviewed by Schulz (1973) and more recent studies include those of Spence (1974), Weingartshofer *et al* (1975), Bose and Linder (1979), Huetz and Mazeau (1983) and Mason and Newell (1986). The assignment of these resonances relies heavily on the analysis of differential cross sections. Despite the amount of data there has not yet been a consistent explanation for the various resonances between 10 and 15 eV.

Theoretically a lot of work has been done on non-resonant differential and integrated cross sections (Arrighini *et al* 1980, Flifet and McKoy 1980, Gibson *et al* 1987,

0953-4075/91/153479+12$03.50

Lima *et al* 1988, Mu-Tao *et al* 1982, Lee *et al* 1990). In contrast there are no calculations of differential cross sections for resonant excitation. Until recently electronic excitation calculations have been restricted to two states for coupled state expansions. These states are represented by single configuration wavefunctions which is often a poor approximation. Test calculations using several coupled channels (da Silva *et al* 1990) and target correlation (Lee *et al* 1990) have been performed in an attempt to improve this model. Recently we have used a six-state (Branchett and Tennyson 1990) and seven-state (Branchett *et al* 1990) model to study integrated electron–H_2 electronic excitation cross sections in both the resonant and non-resonant regions. In these calculations the target states were represented by correlated wavefunctions which yield accurate vertical thresholds for electronic excitation. In this work we extend the previous seven-state integrated cross section calculations of Branchett *et al* (1990), henceforth referred to as I, to differential cross sections. In I the integrated cross sections are in good overall agreement with previous experimental results for all six electronic excitation channels considered. However, the results in I showed considerable structure due to resonances. The available experimental results are not accurate enough to resolve these structures and previous theoretical results cannot produce the detailed structure of the integrated cross sections in this energy region.

2. Method

These calculations were performed using the molecular R-matrix method. The theory for this method has been presented in detail by Gillan *et al* (1987) and Morgan (1990). The R-matrix method divides space into two regions separated by a sphere. Inside the R-matrix sphere full electron–electron Coulomb and exchange interactions are considered. Outside the sphere the interactions are expressed in terms of target multipoles. The target wavefunction is assumed to have negligible amplitude in this region.

In this work we represented the H_2 target by a set of Slater-type orbitals (STO) which are given in I. These orbitals were found by optimization on a series of SCF target calculations. We then represented the seven lowest states of H_2 by a full configuration interaction (CI) representation within the orbital basis set used and with the internuclear separation fixed at 1.4 a_0.

This method gives vertical excitation thresholds that are a good approximation to the very accurate excitation energies obtained from *ab initio* electronic structure calculations. The worst threshold was 0.4 eV in error (see I). In the calculations presented here we shifted the thresholds, and associated diagonal Hamiltonian matrix elements, to correct for these small errors in the excitation thresholds.

Inside the R-matrix sphere the energy-independent wavefunction of scattering plus target electrons is represented by

$$\Psi_k = \mathcal{A}\sum_i a_{i,k}\Phi_i(\boldsymbol{x}_1,\ldots,\boldsymbol{x}_N)F_{i,k}(\boldsymbol{x}_{N+1}) + \sum_j b_{j,k}\phi_j(\boldsymbol{x}_1,\ldots,\boldsymbol{x}_N,\boldsymbol{x}_{N+1}) \qquad (1)$$

where $\mathcal{A}$ is the anti-symmetrization operator and $N = 2$ for an H_2 target. The first term is a sum over target states and continuum functions.

The second term is a sum over configurations where all the electrons are placed in the molecular orbitals belonging to the target. These configurations allow for

high-l terms important in the region of the nuclear singularities, relaxation of the orthogonality condition described below and short range target polarization effects. Because we have used a full CI representation of our H_2 target, we included all possible L^2 configurations in our expansion without risk of over-correlating the continuum electron.

In the inner region the continuum is represented by functions, F_{ik}, expressed as a partial wave expansion about the H_2 centre of mass. These functions were generated as the numerical solutions of the isotropic potential of the SCF target and with the boundary condition of zero derivative at the R-matrix boundary (Gillan *et al* 1987). In this work, as in I, all solutions with $l \leqslant 6$ and $m \leqslant 3$ lying below 5 Ryd were retained. The functions were transformed into an orthonormal set of molecular orbitals by Lagrange orthogonalization (Tennyson *et al* 1987) of the σ_g and π_u sets each to the two lowest target orbitals of the appropriate symmetry, and the σ_u and π_g sets each to the lowest target orbital. The resulting continuum orbitals were then Schmidt orthogonalized to the full set of target orbitals.

R-matrices on the boundary were then constructed from the inner region solutions (Gillan *et al* 1987, Morgan 1990). These R-matrices were then propagated (Morgan 1984) to a radius of 100 a_0. We then used asymptotic expansion techniques (Noble and Nesbet 1984) to obtain solutions to the scattering problem. From these solutions the K-matrices, and hence the T-matrices, were constructed. We retained all the diagonal and off-diagonal dipole and quadrupole moments in the outer region potential expansion. From the T-matrices differential cross sections were calculated using the program of Malegat (1990). In these calculations all symmetries up to $^2\Phi_g$ were included. Other details of the calculation can be found in I.

3. Results

Differential cross sections have been calculated at 50 angles for a range of energies up to 20 eV. Elastic and electronically inelastic processes were considered. Particular emphasis was placed on energies for which experimental data is available and the energies of the resonance features noted in I and summarized in table 1.

Table 1. Resonance positions, E_{res}, and widths, Γ_{res}, for H_2^- with internuclear separation of 1.4 a_0 using a seven-state model of I.

Symmetry	E_{res} (eV)	Γ_{res} (eV)	Assignment
$^2\Sigma_g^+$	10.94	1.24	$1\sigma_g^1\ 1\sigma_u^2$
	12.10	0.106	'a'
$^2\Sigma_u^+$	12.54	0.073	'c' / 'e'
$^2\Pi_u$	12.50	0.018	'c' / 'e'
$^2\Pi_g$	12.80	0.080	'd' ?

Figures 1(a)–1(f) present differential cross sections for elastic collisions in the range 3 eV to 20 eV; the particular energies being chosen to coincide with previous experimental and theoretical results. Full curves give our results including all symmetries up to $^2\Phi_g$. Broken curves give our results summed only up to $^2\Delta_u$ symmetry. In

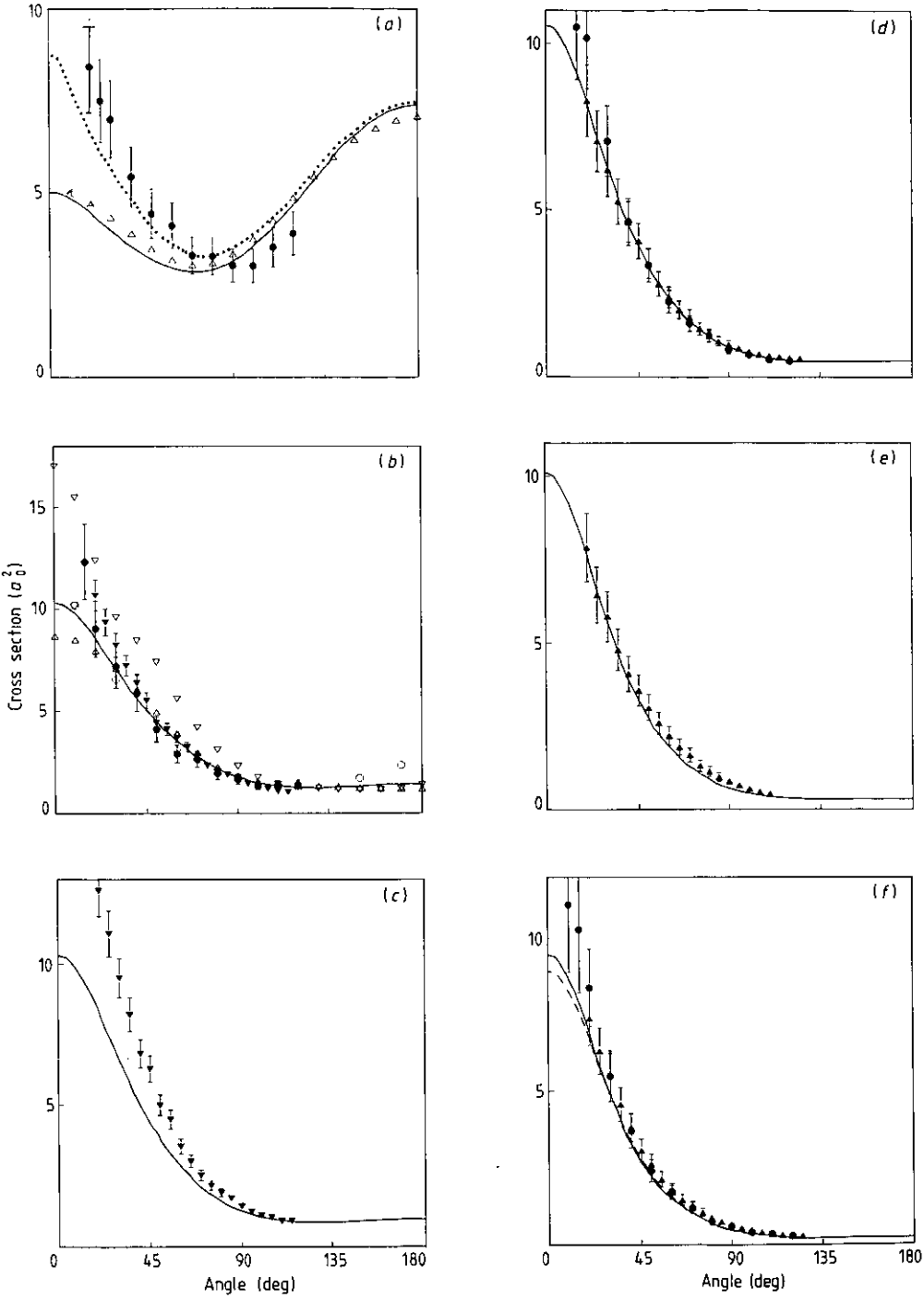

Figure 1. Elastic differential cross section at 3 eV, 10 eV, 12 eV, 15 eV, 17.5 eV and 20 eV. Theory: ——, present work including symmetries up to $^2\Phi_g$; – – –, present work including symmetries up to $^2\Delta_u$; · · · · ·, Snitchler *et al* (1991); ○, Hara (1969); ▽, Truhlar and Brandt (1976) model 3; △, Gibson *et al* (1984). Experiment: ▲, Khakoo and Trajmar (1986a); ●, Nishimura *et al* (1985); ▼, Furst *et al* (1984).

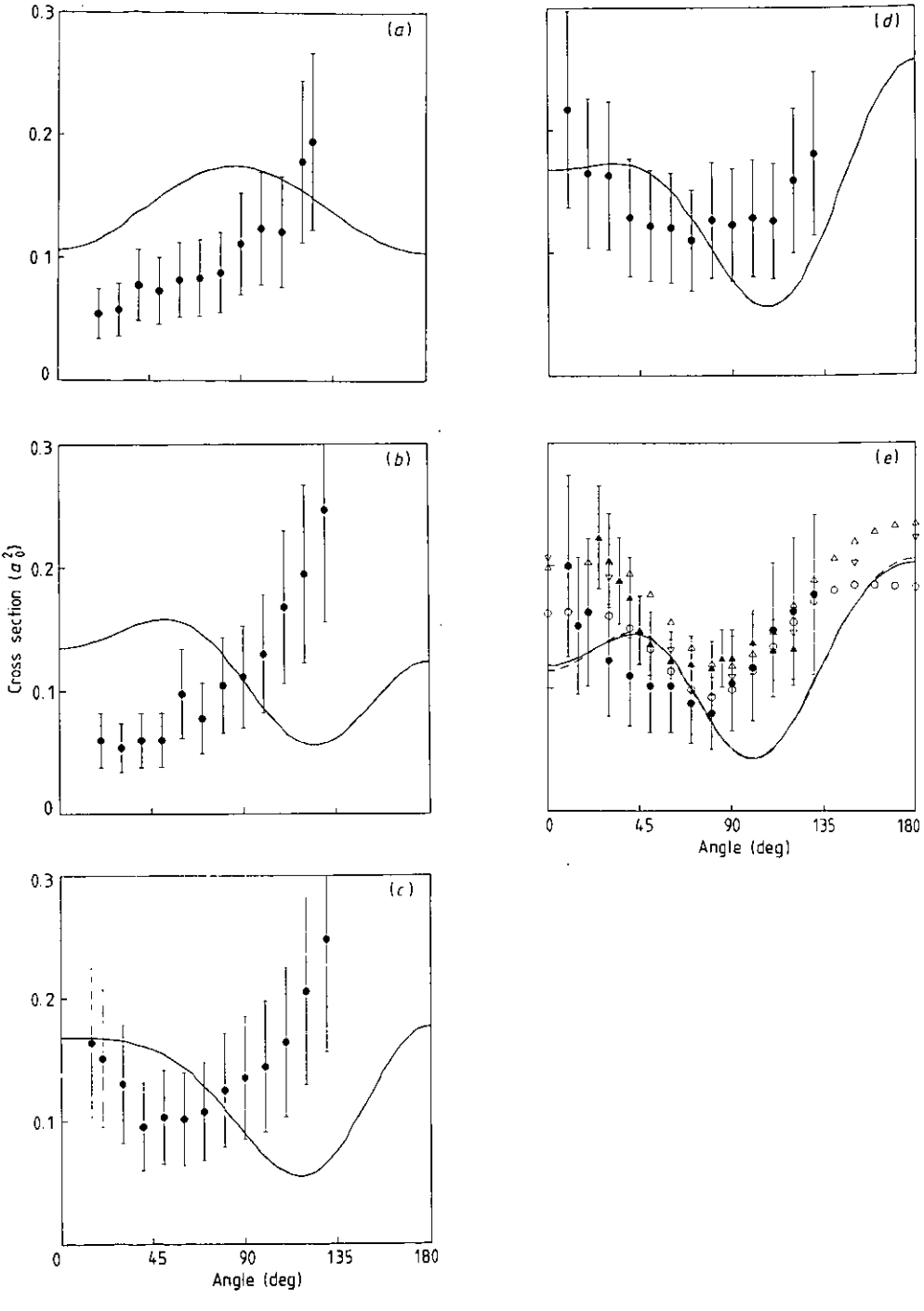

Figure 2. Differential cross sections for excitation to the b $^3\Sigma_u^+$ state at 12 eV, 13 eV, 15 eV, 17 eV and 20 eV. Theory: ——, present work including symmetries up to $^2\Phi_g$; – – –, present work including symmetries up to $^2\Delta_u$; △, Fliflet and McKoy (1980); ○, Lima *et al* (1988); ▽, Lee *et al* (1990). Experiment: ▲, Khakoo *et al* (1987); ●, Nishimura and Danjo (1985).

figures 1(*a*)–1(*e*) these curves are indistinguishable. Figure 2 gives differential cross sections for excitation to the $b\,^3\Sigma_u^+$ state which are compared to previous experimental and theoretical results.

Figure 3 shows the differential cross sections at 20 eV for excitation from the ground to the five higher lying excited states considered in this calculation as a function of angle. The full curves represent the sum over all contributions up to the $^2\Phi_g$ symmetry of the differential cross sections. The broken curves represent the sum over all contributions up to the $^2\Delta_u$ symmetry. Experimental and previous theoretical results are also shown for comparison. This figure presents results at the higher end of the range of incident energies for which our present calculations are valid.

Figure 4 presents differential cross sections as a function of incident energy (excitation functions) at various fixed angles for elastic scattering and for excitation to the $b\,^3\Sigma_u^+$, $a\,^3\Sigma_g^+$ and the $c\,^3\Pi_u$ states. The energy range was chosen to span the resonances listed in table 1. In these figures, the electronic threshold, where the slope of the cross section may be discontinuous, are marked with arrows and the resonance positions are marked with lines.

The differential cross sections at resonance positions are plotted in figure 5. The experimental, electronically elastic (but vibrationally inelastic) results of Joyez *et al* (1973) and the experimental results of Weingartshofer *et al* (1970) for excitation to the $B\,^1\Sigma_u^+$ state have also been plotted for comparison.

4. Discussion

Figure 1 illustrates the good agreement between experimental results and the present work for elastic scattering at energies between 3 eV and 20 eV. The results disagree only for small angles at low energies where our results are less forward peeked; this discrepancy is particularly marked at 3 eV (see figure 1(*a*)). At low energies the results are converged with respect to the number of symmetries included in our calculation. Our results are in excellent agreement with the theoretical results of Gibson *et al* (1984), but agree less well with the calculations of Snitchler *et al* (1991) which agree well with experiment (Brunger *et al* 1991). These latter calculations are an extension of a recent joint experimental/theoretical study on low-energy electron–H_2 collisions (Buckman *et al* 1990). One possible source of error in our calculation is lack of long range polarization effects which are usually introduced into *R*-matrix calculations by using polarized pseudo-states (Gillan *et al* 1988, Danby and Tennyson 1990). However, the $B\,^1\Sigma_u^+$ and $C\,^1\Pi_u$ states included in our close-coupled expansion have a similar effect to the pseudo-states at low energy. Calculations show that our H_2 target has an effective polarisability of 5.172 and 0.809 au for α_0 and α_2 respectively. These compare well with the accurate theoretical values of Kolos and Wolniewicz (1967) of 5.179 and 1.202 au. The source of the discrepancy therefore seems to be lack of vibrational motion. Danby (1991) has shown that at 3 eV that inclusion of vibrational effects can yield results that are typically 12% higher than a rigid rotor model between angles of 0° and 30°. We note also that while Gibson *et al* (1984) and this work were performed within the fixed nuclei approximation, Buckman *et al* (1990) explicitly included both vibrational and rotational motion in their calculations. A detailed study of low-energy behaviour is, however, beyond the scope of the present calculations.

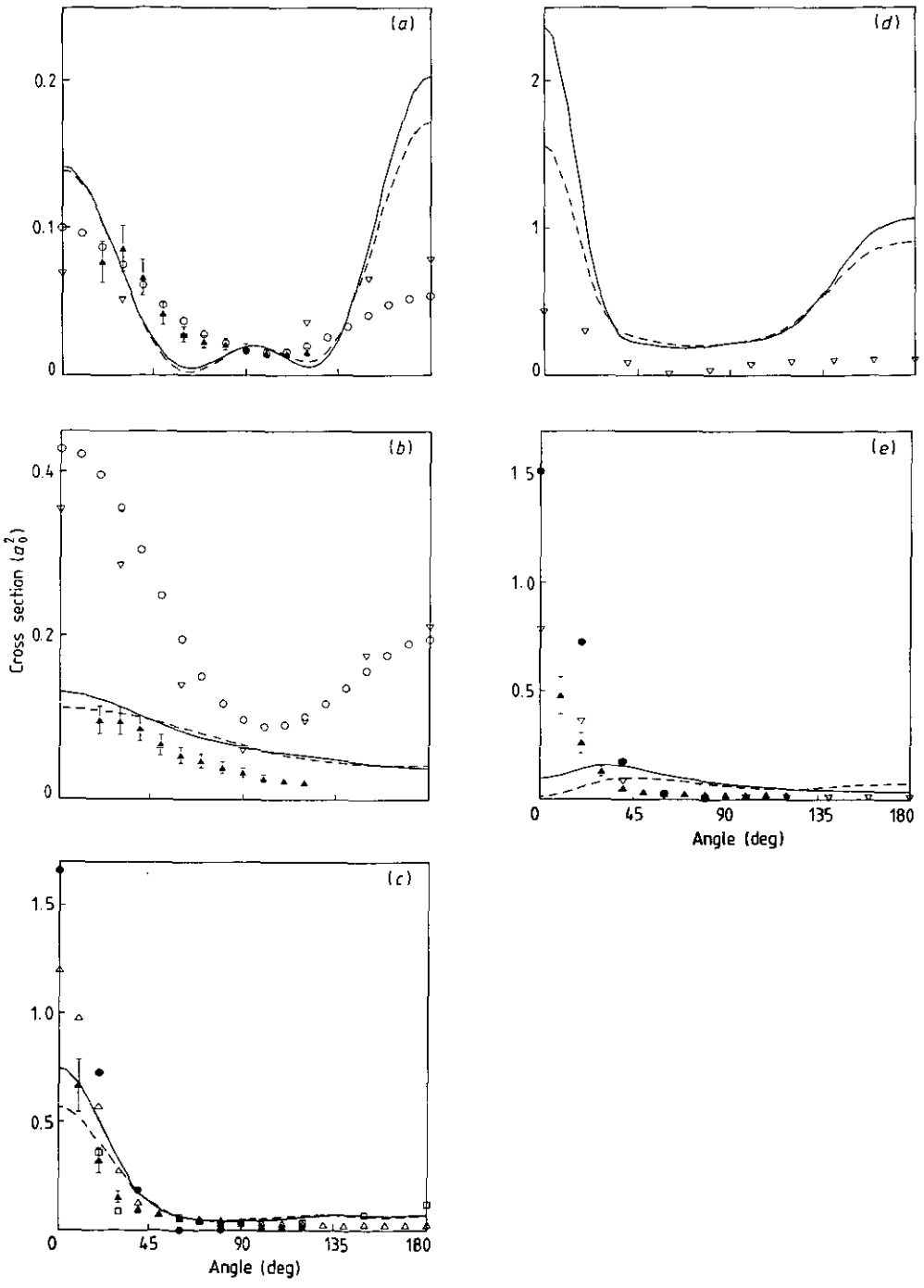

Figure 3. Differential cross sections for electronic excitation to the a $^3\Sigma_g^+$, c $^3\Pi_u$, B $^1\Sigma_u^+$, E,F $^1\Sigma_g^+$ and C $^1\Pi_u$ states at 20 eV. Theory: ——, present work including symmetries up to $^2\Phi_g$; – – –, present work including symmetries up to $^2\Delta_u$; ●, Arrighini *et al* (1980); △, Flifet and McKoy (1980); open square Gibson *et al* (1987); ○, Lima *et al* (1988); ▽, Mu-Tao *et al* (1982) and Lee *et al* (1990). Experiment: ▲, Khakoo and Trajmar (1986b).

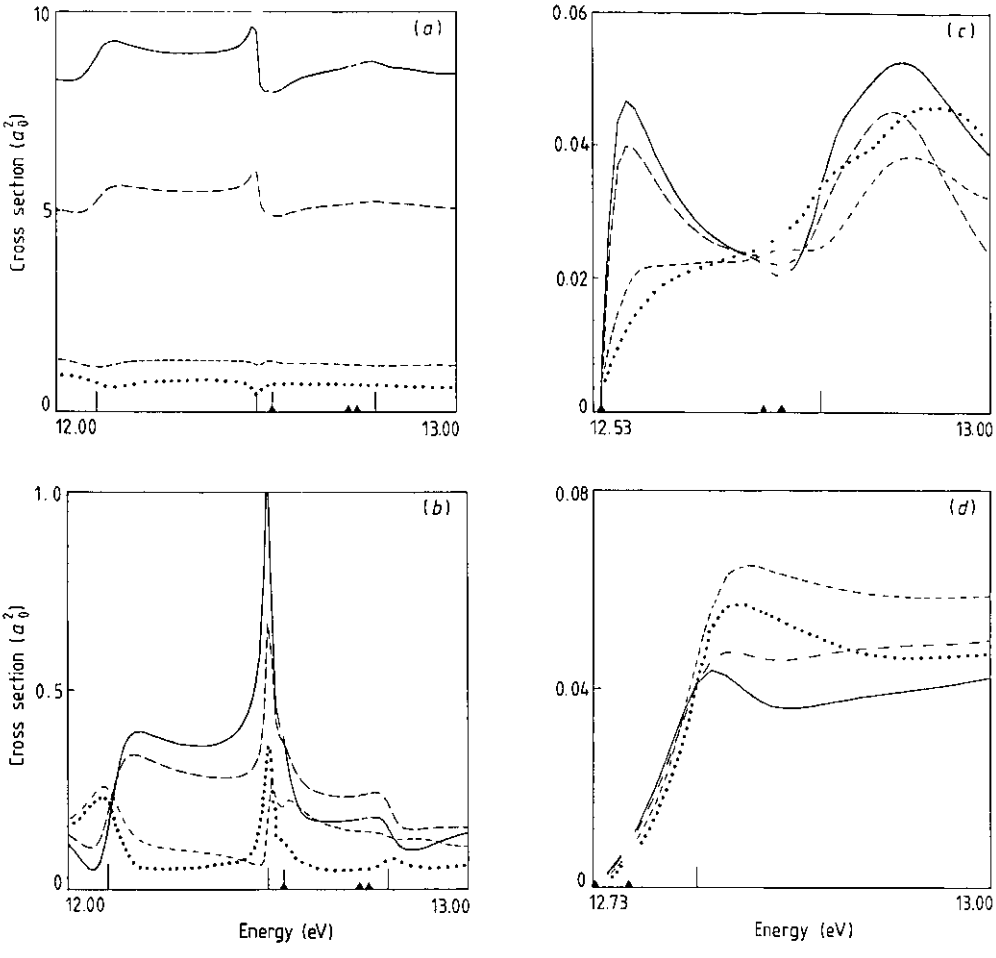

Figure 4. Differential cross sections of energy for elastic scattering and for excitation to the b $^3\Sigma_u^+$, a $^3\Sigma_g^+$ and c $^3\Pi_u$ states. ——, at 120°; – – –, at 90°; - - - -, at 40°; · · · · ·, at 20°. The full triangles on the base line indicate threshold positions and the vertical lines indicate the resonance positions.

At 10 eV (see figure 1(*b*)) our results are in excellent agreement with the experimental results, but at 12 eV (figure 1(*c*)) the agreement is not as good. This is probably caused by the closeness of the resonant energy of 12.10 eV since at higher energies (figures 1(*d*) and 1(*e*)) we are again in excellent agreement with the experimental results. At 20 eV (figure 1(*f*)) there is evidence again that our results are insufficiently forward peaked. Comparison with the results summed up to $^2\Delta_g$ symmetry suggests that this problem is due to our truncation of the number of symmetries explicitly included in the calculation.

The agreement between the present work and the experimental results is not as good for electronic excitation processes shown in figures 2 and 3. The agreement for the $X\,^1\Sigma_g^+ \rightarrow b\,^3\Sigma_u^+$ excitation process (figure 2), the only process for which experimental differential cross sections are available below 20 eV, is worse for the 12 eV (figure 2(*a*)) and 13 eV (figure 2(*b*)) cross sections than for the other energies considered. It is notable that both observed and calculated differential cross sections

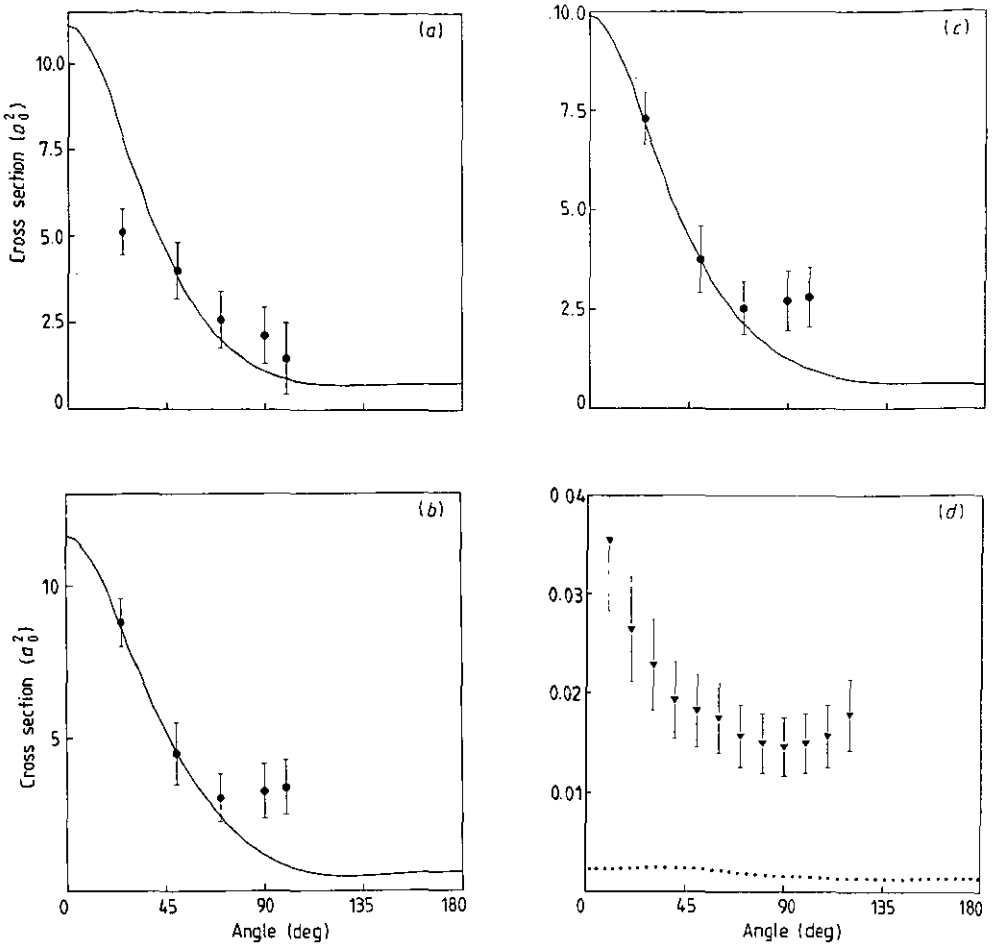

Figure 5. Differential cross sections at the resonant energies of 12.10 eV, 12.50 eV, 12.54 eV and 12.80 eV. This work: ——, elastic scattering; – – –, excitation to the $B\,^1\Sigma_u^+$ state. Experiment: ●, Joyez *et al* (1973) normalized to the 50° data point; ▼, Weingartshofer *et al* (1970).

at these energies are different in shape to those at higher energy. The 12 eV to 13 eV energy region is where several series of resonances have been detected (Schulz 1973). This would make results extremely sensitive to even the smallest energy differences and probably also to the H_2 vibrational motions which have not been considered in the present calculation. At higher energies the present results are close to the experimental results to within experimental error (see figure 2(*d*)). For all the energies considered here the present results have a dip in the differential cross section that is consistently at a larger angle than the experimental results.

For both elastic and inelastic results the convergence with respect to symmetries included is good except at the highest energies. In figure 3 the differential cross sections at 20 eV summed up to $^2\Delta_g$ and up to $^2\Phi_g$ have been plotted for comparison. This lack of convergence leads to only a small underestimation of the cross sections. It would be possible to approximately include the effect of higher symmetries using, for example, the Born approximation (e.g., Norcross and Padial 1982). However, this

approach, which only considers the effect of long-range, spin conserving interactions, would not alter the singlet to triplet excitation cross sections. Since the convergence of our singlet to singlet cross section is not markedly worse than for our singlet to triplet cross section, this approach was deemed inappropriate.

The results shown in figure 3 represent electronic excitation of H_2 considered at the high energy limit of the reliability of this work. The results are, however, in reasonable agreement with previous experimental and theoretical work. Neglect of higher electronic states in the close-coupling expansion implies that our inelastic results overestimate the integrated cross sections at higher energies as loss of flux into these other channels is not allowed for. The present calculations overestimate the differential cross sections for excitation to the $c\,^3\Pi_u$ state (figure 3(*b*)), but this is also partly due to a broad pseudo resonance in the $^2\Pi_u$ symmetry at around 17.5 eV, another effect of the omission of open channels. Higher states of the H_2 target, open or closed, may also be important for polarization or multichannel effects.

For excitation to the $C\,^1\Pi_u$ state at 20 eV (figure 3(*e*)) our results are larger than, but of the same shape as, those of Khakoo and Trajmar (1986b). It can be seen from I that the integrated cross sections of Khakoo and Trajmar (1986b) were also lower than the theoretical predictions for this symmetry at 20 eV, but that the experimental results of Ajello *et al* (1984) were in much better agreement with the theory. Differential cross section results of Ajello *et al* (1984) are not, however, available for comparison.

Other previous attempts to calculate differential cross sections at 20 eV are given in figure 3. Our results generally improve on these. Thus, for example, both the shape and magnitude of differential cross section for $X\,^1\Sigma_g^+ \rightarrow c\,^3\Pi_u$ (figure 3(*b*)) are in significantly better agreement with experiment than the previous calculations (Lima *et al* 1988, Lee *et al* 1990).

The graph of excitation to the $a\,^3\Sigma_g^+$ state (figure 3(*a*)) shows clearly the difficulties in obtaining integrated cross sections by extrapolating data recorded over a limited range of angles. It would be almost impossible to extrapolate accurately to small or large angles by considering only the results between 45° and 135°.

Differential cross section as a function of energy at several angles are presented in figure 4. It can be seen that the shape, as well as the magnitude, of the differential cross section varies depending on the angle at which it is observed, both for elastic and inelastic collisions. Indeed for excitation to the $b\,^3\Sigma_u^+$ (figure 4(*b*)) at energies around 12.05 eV the differential cross section is forward peaked, but at higher energies it becomes backward peaked. The target state thresholds are also marked, but it can be seen that these do not have a dramatic effect on the differential cross sections. However, the positions of the resonances can be clearly seen for both elastic and inelastic collisions (see for example figures 4(*a*) and 4(*b*)). It can be seen that the apparent resonance width and position vary not only with the angle of observation, but also with the exit channel considered. This is in agreement with the observation of Huetz and Mazeau (1983). Indeed for elastic scattering (figure 4(*a*)) the resonance at 12.80 eV does not appreciably affect the shape of the differential cross section at any of the angles considered, but for excitation to the $b\,^3\Sigma_u^+$ state (figure 4(*b*)) this is clearly not the case.

Figure 5 shows the differential cross section as a function of angle for the 'a', 'c' / 'e', 'c' / 'e' and 'd' resonant energies respectively (see table 1 for resonance assignments and I for a discussion of these resonances). It can be seen that the shapes of the distributions vary according to which exit channel is considered and the max-

ima in energies are different for each exit channel. It can also be seen that the angular asymptotic distributions do not in general correspond to the shape of the lowest partial wave contributing to a particular resonance. In particular only the differential cross section for excitation to the $b\,^3\Sigma_u^+$ at 12.10 eV (not shown) is approximately symmetric about 90° suggesting that the distribution could be dominated by one partial wave. None of the distributions in figure 5 have this symmetry and therefore cannot be approximated by a single predominant partial wave, but rather a combination of several partial waves. The agreement between the present results and the electronically elastic, but rotationally and vibrationally inelastic experimental results of Joyez *et al* (1973) (figures 5(*a*), 5(*b*) and 5(*c*)), normalized to the 50° data point, is therefore good. The agreement between the electronically and vibrationally inelastic experimental results of Weingartshofer *et al* (1970) with the present results is not so good (see figure 5(*d*)). Although the general shape of the distributions is similar our results greatly underestimate the experimental results.

It should be remembered that for this work the internuclear separation was fixed at 1.4 a_0 removing all vibrational effects. These effects are probably most important in the resonance region where they may lead to large differences in the integrated cross sections. The effect of including vibrational motion on the differential cross sections in this region remains to be investigated.

5. Conclusions

We have presented differential cross sections for scattering energies up to 20 eV for electron–H_2 collisions using seven coupled electronic states of H_2 represented by accurate, correlated wavefunctions. The resonant and non-resonant calculations are compared with previous theoretical and experimental results.

Excellent agreement for elastic differential cross section is obtained in the 10 eV to 20 eV range. For the inelastic processes, all of which have significantly smaller integrated cross sections, the agreement can only be described as moderate. Given the sophistication of the present calculation this is somewhat disappointing. It is therefore worthwhile considering what aspects of these calculations need improving if better results are to be achieved.

The calculations neglect many electronic channels (including ionization) that are open at 20 eV. This may have several consequences: overestimation of integrated excitation cross sections to compensate for the lack of channels taking flux from the calculation; neglect of short-range polarization or multichannel effects; the occurrence of pseudo-resonances. Although we can tell that pseudo-resonances are not a major source of error, it is hard to quantify the other two effects without performing further, more elaborate, calculations. Finally, our calculations were performed for a single internuclear separation. At energies in the resonance region one would expect the differential cross sections to be sensitive to vibrational motion. Neglecting this is probably the major source of error in the present calculations.

Our calculations of differential cross sections in the resonance region illustrate that the analysis of these resonances by monitoring a single exit channel must be performed with caution. We find large variations in the shape of differential cross section according to the exit channel monitored. Furthermore, the resonances peak positions are also a function of the channel and angle monitored.

Acknowledgments

We thank Grahame Danby and Nigel Mason for helpful discussions during the course of this work. This work was supported by Science and Engineering Research Council grant GR/F/14550.

References

Ajello J M, Shemansky D, Kwok T L and Yung Y L 1984 *Phys. Rev.* A **29** 636–53
Arrighini G P, Biondi F and Guidotti C 1980 *Mol. Phys.* **41** 1501–14
Bose and Linder 1979 *J. Phys. B: At. Mol. Phys.* **12** 3805–17
Branchett S E and Tennyson J 1990 *Phys. Rev. Lett.* **64** 2889–92
Branchett S E, Tennyson J and Morgan L A 1990 *J. Phys. B: At. Mol. Opt. Phys.* **23** 4625–39
Buckman S J, Brunger M J, Newman D S, Snitchler G, Alston S, Norcross D W, Morrision M A, Saha B C, Danby G and Trail W K 1990 *Phys. Rev. Lett.* **65** 3253–6
Brunger M J, Buckman S J, Newman D S and Alle D T 1991 *J. Phys. B: At. Mol. Opt. Phys.* **24** 1435–48
da Silva A R J, Lima M A P, Brescansin L M and McKoy V 1990 *Phys. Rev.* A **41** 2903–5
Danby G 1991 Private communication
Danby G and Tennyson J 1990 *J. Phys. B: At. Mol. Opt. Phys.* **23** 1005–16
Fliflet A W and McKoy V 1980 *Phys. Rev.* A **21** 1863–75
Furst J, Mahgerefteh M and Golden D E 1984 *Phys. Rev.* A **30** 2256–60
Gibson T L, Lima M A P, McKoy V and Huo W M 1987 *Phys. Rev.* A **35** 2473–8
Gibson T L, Lima M A P, Takatsuka K and McKoy V 1984 *Phys. Rev.* A **30** 3005–11
Gillan C J, Nagy O, Burke P G, Morgan L A and Noble C J 1987 *J. Phys. B: At. Mol. Phys.* **20** 4585–603
Gillan C J, Noble C J and Burke P G 1988 *J. Phys. B: At. Mol. Opt. Phys.* **21** L53–9
Hara S 1969 *J. Phys. Soc. Japan* **27** 1009–19
Huetz A and Mazeau J 1983 *J. Phys. B: At. Mol. Phys.* **16** 2577–92
Joyez G, Comer J and Read F H 1973 *J. Phys. B: At. Mol. Phys.* **6** 2427–40
Khakoo M A and Trajmar S 1986a *Phys. Rev.* A **34** 138–45
—— 1986b *Phys. Rev.* A **34** 146–56
Khakoo M A, Trajmar S, McAdams R and Shyn T W 1987 *Phys. Rev.* A **35** 2832–7
Kolos W and Wolniewicz L 1967 *J. Chem. Phys.* **46** 1426–32
Lee M-T, Machado L E, Leal E P, Brescansin L M, Lima M A P and Machado F B C 1990 *J. Phys. B: At. Mol. Opt. Phys.* **23** L233–7
Lima M A P, Gibson T L, McKoy V and Huo W M 1988 *Phys. Rev.* A **38** 4527–36
Malegat L 1990 *Comput. Phys. Commun.* **60** 391–404
Mason N J and Newell W R 1986 *J. Phys. B: At. Mol. Phys.* **18** L203–7
Morgan L A 1984 *Comput. Phys. Commun.* **31** 419–22
—— 1990 *Proc. 16th Int. Conf. on Physics of Electronic and Atomic Collisions* ed A Dalgarno, R S Freund, M S Lubell and T B Lucatorto (New York: Plenum) Invited Papers and Progress Reports pp 96–102
Mu-Tao L, Lucchese R R and McKoy V 1982 *Phys. Rev.* A **26** 3240–8
Nishimura N and Danjo 1986 *J. Phys. Soc. Japan* **55** 3031–6
Nishimura N, Danjo A and Sugahara H 1985 *J. Phys. Soc. Japan* **54** 1757–68
Noble C J and Nesbet R K 1984 *Comput. Phys. Commun.* **33** 399–411
Norcross D W and Padial N T 1982 *Phys. Rev.* A **25** 226–238
Schulz G J 1973 *Rev. Mod. Phys.* **45** 423–86
Snitchler G, Alston S, Norcross D, Saha B, Danby G, Trail W and Morrison M A 1991 Private communication
Spence D 1974 *J. Phys. B: At. Mol. Phys.* **7** L87–90
Tawara H, Itikawa Y, Nishimura N and Yoshimo M 1990 *J. Phys. Chem. Ref. Data* **19** 617–36
Tennyson J, Burke P G and Berrington K A 1987 *Comput. Phys. Commun.* **47** 207–16
Truhlar D G and Brandt M A 1976 *J. Chem. Phys.* **65** 3092–3101
Weingartshofer A, Clarke E M, Holmes J K and McGowan J W 1975 *J. Phys. B: At. Mol. Phys.* **8** 1552–69
Weingartshofer A, Ehrhardt H, Hermann V and Linder F 1970 *Phys. Rev.* A **2** 294–304